Hydrothermal Synthesis

DOI: 10.1002/anie.200702519

Uniform Nanostructured Arrays of Sodium Rare-Earth Fluorides for Highly Efficient Multicolor Upconversion Luminescence**

*Fan Zhang, Ying Wan, Ting Yu, Fuqiang Zhang, Yifeng Shi, Songhai Xie, Yigang Li, Lei Xu, Bo Tu, and Dongyuan Zhao**

Upconversion (UC) phosphors emit high-energy photons when they are excited by low-energy photons. This property is attractive for flat-panel displays,[1,2] optical storage,[3] biolabels,[4] solid-state lasers,[5] and light-emitting diodes.[6] High UC luminescence efficiency is typically generated by bulk materials[1] and colloidal nanocrystals[7] of hexagonal-phase lanthanide-doped rare-earth fluorides, but nanoarrays of single crystals are more desirable for solid-state lasers. The UC luminescence efficiency can be enhanced if the nanoarrays are aligned with photonic-crystal microstructures, and the faceted end planes of well-shaped crystals serve as good laser-cavity mirrors.[8]

Herein, we report a general solution-based approach for the preparation of uniform nanostructured arrays of the sodium rare-earth (M) fluorides $NaMF_4$. The arrays can be prepared with well-controlled morphologies (tubes, disks, or rods), phases (cubic or hexagonal), sizes (80–900 nm), and compositions. This approach avoids the assistance of templates, applied fields, and undercoating on substrates,[9,10] and is industrially feasible, owing to its ease and low cost. Multicolor UC fluorescence is also generated when the nanoarrays are pumped in the near-infrared (NIR) region; for example, green or blue fluorescence is produced for nanoarrays of $NaYF_4$ codoped with Yb^{3+} and Er^{3+}, or Yb^{3+} and Tm^{3+}, respectively. Owing to their unique luminescence and chemical flexibility, these nanoarrays offer great potential as light sources for miniaturized solid-state lasers.

The nanostructured arrays of $NaMF_4$ were prepared by a facile hydrothermal approach, using oleic acid as a stabilizing agent, and NaF and $M(NO_3)_3$ as precursors, in the temperature range of 130–230 °C under basic conditions (for details see the Supporting Information). The products are composed of uniformly hexagonal nanotubes with outer diameters of about 250 nm and lengths of about 500 nm, as shown by scanning electron microscopy (SEM) (Figure 1a).

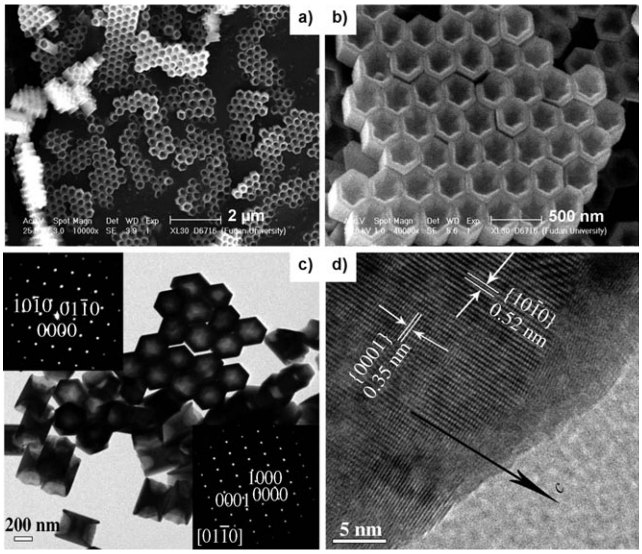

Figure 1. a),b) SEM images of arrays of hexagonal nanotubes of β-$NaYF_4$. c) TEM image of the nanotubes and corresponding ED patterns (insets). d) HRTEM image of a nanotube.

Energy-dispersive X-ray (EDX) analyses of the products obtained using $Y(NO_3)_3$ as a precursor revealed that the nanotubes have a molar Na/Y/F ratio of 1.0:1.0:4.0, demonstrating the formation of stoichiometric $NaYF_4$ (see Figure S1 in the Supporting Information). Owing to their homogeneity, these tubes could pack into ordered hexagonal arrays (Figure 1b). Inside the hexagonal tubes are wedge-shaped instead of channel structures, as confirmed by transmission electron microscopy (TEM) (Figure 1c). Electron diffraction (ED) patterns taken from top/bottom surfaces and side faces of the tubes could be indexed as {0001} and $\{1\bar{1}00\}$ planes, respectively, of hexagonal β-$NaYF_4$ (space group $P6_3/mmc$; Figure 1c, inset). The nanotubes grow along the [0001] direction, owing to the aspect ratio of the cell parameters. High-resolution (HR) TEM images show interplanar spacings

---

[*] F. Zhang, T. Yu, Dr. F. Q. Zhang, Dr. Y. F. Shi, Dr. S. H. Xie, Dr. B. Tu, Prof. Dr. D. Y. Zhao
Laboratory of Advanced Materials
Shanghai Key Laboratory of Molecular Catalysis and Innovative Materials
Department of Chemistry
Fudan University, Shanghai 200433 (China)
Fax: (+86) 21-5566-4192
E-mail: dyzhao@fudan.edu.cn
Homepage: http://homepage.fudan.edu.cn/~dyzhao/default.htm
Dr. Y. Wan
Department of Chemistry
Shanghai Normal University, Shanghai 200234 (China)
Dr. Y. G. Li, Prof. Dr. L. Xu
Department of Optical Science and Engineering
Fudan University, Shanghai 200433 (China)

[**] This work was supported by the NSF of China (20421303 and 20521140450), the State Key Basic Research Program of China (2006CB202502 and 2006CB0N0302), the Shanghai Science and Technology Committee (06DJ14006, 055207078, and 05DZ22313), and the Shanghai Nanotech Promotion Center (0652nm024). We thank J. Shan, D. R. Wang, H. Y. Chen, and Y. Chen for assistance with the characterization.

Supporting information for this article is available on the WWW under http://www.angewandte.org or from the author.

of 0.52 and 0.35 nm corresponding to the $\{10\bar{1}0\}$ and $\{0001\}$ planes of β-NaYF$_4$, respectively (Figure 1 d).

An important feature of the nanotubes is that their concave surface also possesses a sixfold structure associated with the crystal symmetry. X-ray diffraction (XRD) patterns further indicate that the nanotubes obtained after heating at 230 °C for 12 h consist of pure β-NaYF$_4$ (Figure S2).

The XRD patterns demonstrate that the products obtained with lower NaOH concentrations remain nanocrystals of β-NaYF$_4$ (Figure S3). SEM images reveal that the products obtained by decreasing the concentration of NaOH to some extent consist of fairly uniform disks with diameters of about 800 nm and thicknesses of about 300 nm (Figure 2 a), which close pack into nanoarrays in some domains (Figure 2 b). All the disks feature flower-like patterns, with a sixfold axis, on their tops and bottoms. Careful statistical measurements reveal that the rotary direction of the flower patterns is random. The number of disks with left-handed patterns is equal to that with right-handed patterns. For individual disks, only one rotary direction is observed in TEM images (Figure 2 c and Figure S4 a), which indicates that the top and bottom faces of the disks have opposite rotation patterns. This result may explain the even distribution of right- and left-handed patterns (Figure 2 d). The side faces of the disks exhibit a well-faceted quasirhombic morphology (Figure 2 a,b,d and Figure S4 b). ED patterns verify that the hexagonal disks are single crystals of the β-NaYF$_4$ structure with $\{0001\}$ top/bottom surfaces and $\{1\bar{1}00\}$ side faces (Figure 2 c, inset, and Figure S4 c,d). The $\{1000\}$ lattice fringe estimated from an HRTEM image is 0.52 nm (Figure 2 e), in good agreement with the value of 0.52 nm calculated from XRD data (Figure S3).

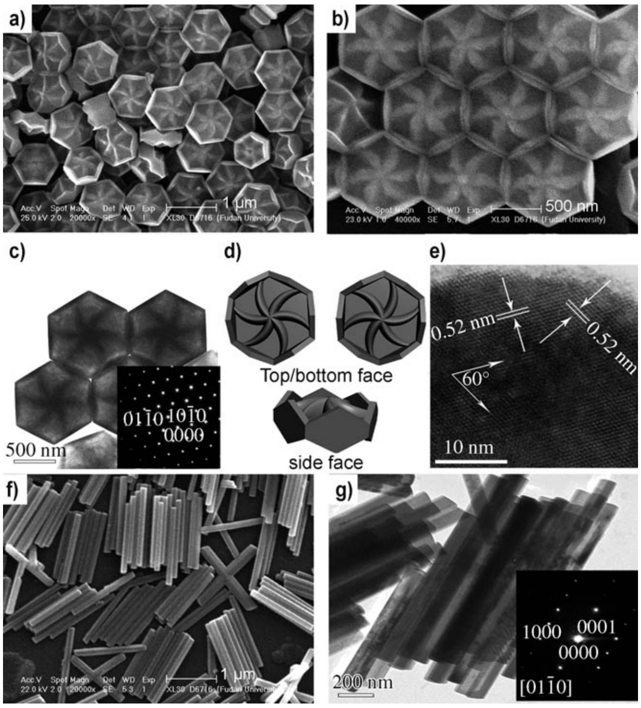

Figure 2. a),b) SEM images of arrays of flower-patterned hexagonal disks of β-NaYF$_4$. c) TEM image of the disks and corresponding ED pattern (inset). d) Illustration of the $\{0001\}$ top/bottom faces and the $\{1\bar{1}00\}$ side faces of a disk. e) HRTEM image of a corner of a disk. f) SEM image of arrays of hexagonal nanorods of β-NaYF$_4$. g) TEM image of the nanorods and corresponding ED pattern (inset).

At higher NaF concentrations, nanorods of β-NaYF$_4$ can be obtained. SEM and TEM images show that these nanorods have uniform diameters of about 110 nm and lengths of about 2 µm (Figure 2 f,g). The same β-NaYF$_4$ structure as for the nanotubes and disks was detected for the nanorods by XRD, HRTEM, and ED analyses. Again, the top/bottom surfaces could be indexed as $\{0001\}$ planes and the side faces as $\{1\bar{1}00\}$ planes (Figure 2 g, inset, and Figure S5). The intensity of the 100 diffraction peak in the XRD pattern is relatively high, consistent with preferential growth along the [0001] direction.

Temperature and time of the hydrothermal reaction greatly influence the final products. A mixture of the cubic α-NaYF$_4$ (space group $Fm\bar{3}m$) phase and the hexagonal β-NaYF$_4$ phase was obtained after hydrothermal reaction at 230 °C for 1 h, as shown in the XRD pattern of the products (Figure S6 in the Supporting Information). TEM images and ED patterns, indeed, show both large cylindrical particles of the hexagonal phase and small nanocrystals of the cubic phase (Figure S7 in the Supporting Information). Prolonging the reaction time (3–24 h) results in the formation of increasing amounts of hexagonal nanotubes and eventually yields pure β-NaYF$_4$. Nanocrystals of cubic α-NaYF$_4$ with diameters of about 5 nm are formed at a low temperature of 130 °C (Figure S2 and Figure S8). Increasing the reaction temperature leads to a phase transformation from α- to β-NaYF$_4$ (Figure S2 in the Supporting Information).

The phase and morphology of the products can also be tuned by adjusting the composition of the reaction mixture. With an increase in the oleic acid/NaOH ratio, a phase transformation from the cubic phase to the hexagonal phase occurs as well. Under these conditions, a short reaction time (9 h) results in flower-patterned disks of β-NaYF$_4$ with unclear rotary directions and very small side faces (Figure S9 a). Comparison with the disks obtained after a 12-hour hydrothermal treatment, which have distinct rotary directions, suggests that the rotary direction is generated from competition between the [0001] and $[01\bar{1}0]$ directions in the growth of the $\{1\bar{1}00\}$ side faces. Further growth of the side faces along the [0001] direction leads to the dislocation of the flower-pattern ends. When the concentration of Y^{3+} (with Y^{3+}/F^- constant at 1:4) increases from 0.2 to 0.8 to 1.6 mM, the outer diameter of the β-NaYF$_4$ nanotubes increases from 80 to 200 to 500 nm (Figure S9 b–d). The present synthesis approach is general and can produce nanoarrays of hexagonal NaMF$_4$ phases with other rare earths, such as NaErF$_4$, NaTmF$_4$, NaYbF$_4$, and NaLuF$_4$ (Figure S10).

We speculate that the formation of NaYF$_4$ is related to a dissolution–reconstruction process (Figure 3),[11] in which α-NaYF$_4$ is a metastable phase, and the transformation from α- to β-NaYF$_4$ is irreversible. The reaction system could be described with a model of microemulsion and reverse micelles (Figure 3). The sodium oleate generated from oleic acid and NaOH forms reverse micelles containing Y^{3+} ions. These reverse micelles, together with NaF, oleic acid, and water,

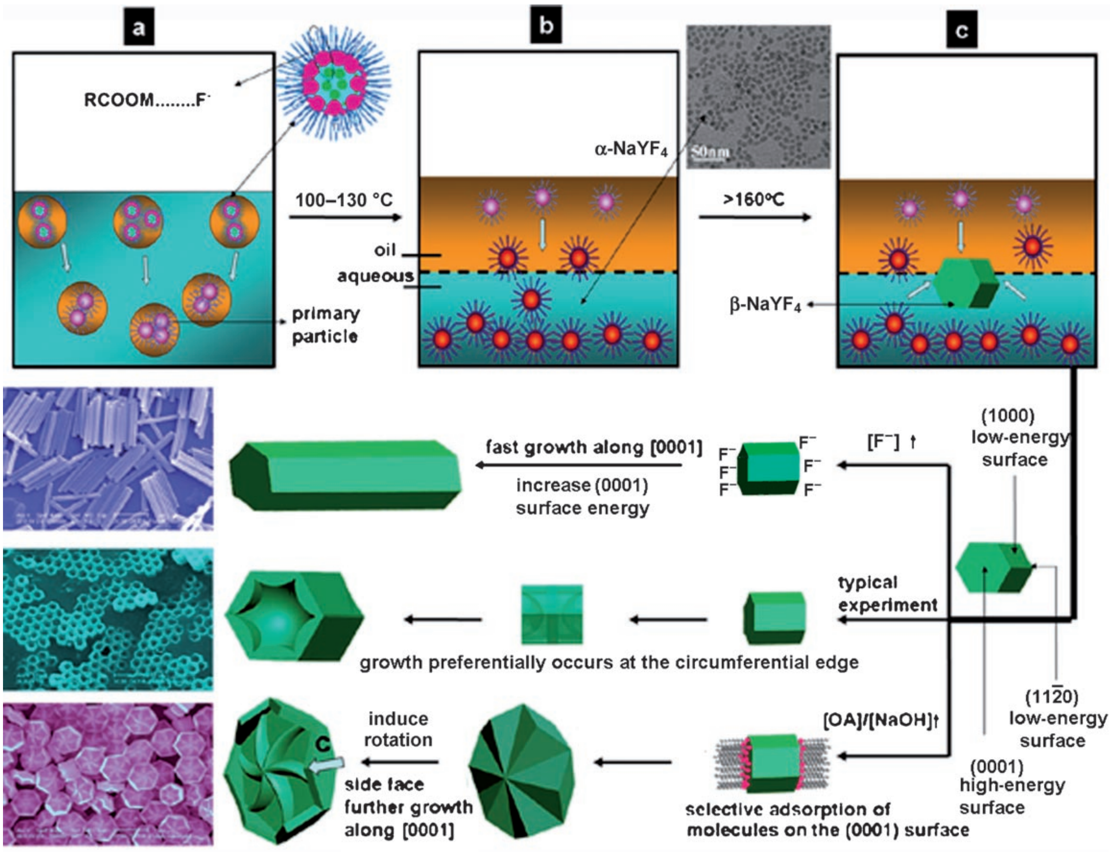

Figure 3. Schematic diagram of the proposed process for the formation of arrays of nanocrystals of α-$NaYF_4$ and β-$NaYF_4$. See text for details.

form a microemulsion.[12] The oleate anions have metal-coordinating and solvophilic groups. The carboxy groups are typically electron donors and could coordinate with electron-poor metal atoms at the surfaces of the nanocrystals. The Y^{3+} ions in the reverse micelles could, therefore, react with oleate groups and F^- ions simultaneously (Figure 3a). In the low-temperature range of 100–130 °C, discrete α-$NaYF_4$ nanocrystals with uniform size are readily formed by using reverse micelles as confined reactors (Figure 3b). When the temperature is above 160 °C, cylindrical β-$NaYF_4$ seeds quickly nucleate and grow. The simultaneous formation of α- and β-$NaYF_4$ nanoparticles at higher temperatures consumes most reactants (Figure 3c). Therefore, a dissolution–reconstruction process occurs to form the final β-$NaYF_4$ products with different morphologies.

The growth of β-$NaYF_4$ crystals tends to occur along the [0001] direction with a cylindrical morphology, owing to the anisotropic crystal structure.[13] The formation of tubes can be attributed to a dissolution–reconstruction process of β-$NaYF_4$ occurring at the circumferential edge of each cylindrical seed.[14] Subsequent fast growth on the edges leads to a depletion of substances in the centers and eventually produces single-crystal tubes of β-$NaYF_4$ with well-defined cross sections. If the oleic acid/NaOH ratio is increased, the selective adsorption of organic molecules may inhibit the growth of the {0001} faces. Accordingly, the growth trend is along the perpendicular [1000] direction, resulting in disk-shaped crystals.[15] In addition, an increase in the F^- concentration may improve the dissolution–reconstruction process. The preferential growth along the [0001] direction results in nanorods with high aspect ratios.

The visible luminescence spectra of nanorod arrays of β-$NaYF_4$ codoped with 2 wt % Er^{3+} and 20 wt % Yb^{3+} display two emission bands under infrared excitation, which can be assigned to the 4f–4f transitions of the Er^{3+} ions (Figure 4a and Figure S11). A dominant red emission originating from the $^4F_{9/2}\rightarrow{}^4I_{15/2}$ transition is observed at 630–680 nm.[16] The green luminescence at 510–570 nm is attributed to the $^2H_{11/2},{}^4S_{3/2}\rightarrow{}^4I_{15/2}$ transition (Figure S12). Compared with a bulk sample of Er^{3+}/Yb^{3+}-doped $NaYF_4$ prepared by the coprecipitation method, which shows a ratio of red to green photons of 1:1.7, the present nanorods show a higher ratio of 1.9:1, which may be related to their uniform size.[17]

Nanorods of β-$NaYF_4$ codoped with 2 wt % Tm^{3+} and 20 wt % Yb^{3+} exhibit two visible luminescence bands at 450–490 and 630–680 nm, which are ascribed to the blue-emission $^1G_4\rightarrow{}^3H_6$ transition and the weak red-emission $^1G_4\rightarrow{}^3F_4$ transition, respectively (Figure 4b). An intense near-infrared emission at 750–850 nm is due to the $^3H_4\rightarrow{}^3H_6$ transition. Figure 4c shows photographs of visible upconversion luminescence in hexane solutions of $NaYF_4$ with 2 % Er^{3+} and 20 % Yb^{3+} and of $NaYF_4$ with 2 % Tm^{3+} and 20 % Yb^{3+} excited with a laser at 978 nm. The highly efficient emission luminescence clearly demonstrates that the nanostructured arrays with controlled shapes are excellent upconversion host materials. The luminescence intensity of the nanorods syn-

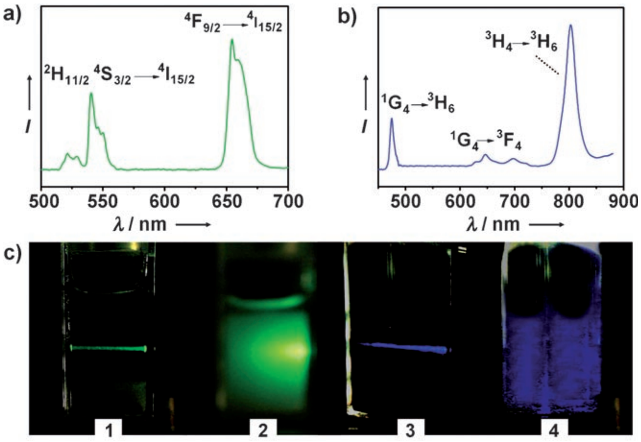

Figure 4. UC luminescence spectra of β-NaYF$_4$ codoped with a) 2 wt% Er^{3+} and 20 wt% Yb^{3+}, or b) 2 wt% Tm^{3+} and 20 wt% Yb^{3+} (excited with a 978-nm laser diode; power density of 80 W cm^{-2}). c) Photographs of the UC luminescence of 0.2 wt% (1) and 1 wt% (2) hexane solutions of β-NaYF$_4$ codoped with 2 wt% Er^{3+} and 20 wt% Yb^{3+}, and of 0.2 wt% (3) and 1 wt% (4) hexane solutions of β-NaYF$_4$ codoped with 2 wt% Tm^{3+} and 20 wt% Yb^{3+} (excited with a 978-nm laser diode; laser power of 800 mW).

thesized with high F$^-$ concentrations is stronger than those of the tube and disk samples. This result may be related to the large amount of F$^-$ ions on the surface of the nanorods, which could prevent oxygen contamination.

These results illustrate the great potential of well-defined nanoarrays of tubes and rods of β-NaYF$_4$ for use in laser-cavity mirrors and laser media. The arrays of β-NaYF$_4$ nanoparticles could shed light for the optical microdisk resonator, which could confine light to a small modal volume by resonant recirculation with a low optical loss. We consider this an important step towards the development of upconversion nanostructured materials with a great potential for the development of miniature optoelectronics, in particular in the fields of solid-state lasers, photonic crystals, optical storage, and waveguides.

Received: June 10, 2007
Revised: July 16, 2007

Keywords: fluorides · hydrothermal synthesis · luminescence · nanostructures · rare earth metals

---

[1] E. Downing, L. Hesselink, J. Ralston, R. Macfarlane, *Science* **1996**, *273*, 1185.
[2] P. Lodahl, A. F. van Driel, I. S. Nikolaev, A. Irman, K. Overgaag, D. Vanmaekelbergh, W. L. Vos, *Nature* **2004**, *430*, 654.
[3] P. Cheben, F. del Monte, D. J. Worsfold, D. J. Carlsson, C. P. Grover, J. D. Mackenzie, *Nature* **2000**, *408*, 64.
[4] D. van de Rijke, H. Zijlmans, S. Li, T. Vail, A. K. Raap, R. S. Niedbala, H. J. Tanke, *Nat. Biotechnol.* **2001**, *19*, 273.
[5] G. Rumbles, *Nature* **2001**, *409*, 572.
[6] M. Stockman, *Nat. Mater.* **2004**, *3*, 423.
[7] G. S. Yi, H. C. Lu, S. Y. Zhao, G. Yue, W. J. Yang, *Nano Lett.* **2004**, *4*, 2191.
[8] M. H. Huang, S. Mao, H. Feick, H. Q. Yan, Y. Y. Wu, H. Kind, E. Weber, R. Russo, P. D. Yang, *Science* **2001**, *292*, 1897.
[9] B. Z. Tian, X. Y. Liu, B. Tu, C. Z. Yu, J. Fan, L. M. Wang, S. H. Xie, G. D. Stucky, D. Y. Zhao, *Nat. Mater.* **2003**, *2*, 159.
[10] X. Wang, J. Zhuang, Q. Peng, Y. D. Li, *Nature* **2005**, *437*, 121.
[11] J. W. Mullin, *Crystallization*, 3rd ed., Butterworth-Heinemann, Oxford, **1997**.
[12] M. Li, H. Schnablegger, S. Mann, *Nature* **2000**, *402*, 393.
[13] Y. W. Jun, J. S. Choi, J. Cheon, *Angew. Chem.* **2006**, *118*, 3492; *Chem. Int. Ed.* **2006**, *45*, 3414.
[14] B. Mayers, Y. N. Xia, *Adv. Mater.* **2002**, *14*, 279–282.
[15] X. G. Peng, L. Manna, W. D. Yang, J. Wickham, A. P. Alivisatos, *Nature* **2000**, *404*, 59.
[16] F. Auzel, *Chem. Rev.* **2004**, *104*, 139.
[17] R. H. Page, K. I. Schaffers, P. A. Waide, J. B. Tassano, S. A. Payne, *J. Opt. Soc. Am. B* **1998**, *15*, 996.